Applied Physics Research; Vol. 15, No. 2; 2023
ISSN 1916-9639 E-ISSN 1916-9647
Published by Canadian Center of Science and Education

Symmetric Fano Profiles of Two-photon Electronic Transitions Observed in an Ultracold Rydberg Gas

Jianing Han[1], Brianna Provencher[1], Juliet Mitchell[1], Chandler Steade[2], Na Gong[2] & Jinhui Wang[2]

[1]Department of Physics, University of South Alabama, Mobile, Alabama, USA
[2]Department of Electrical and Computer Engineering, University of South Alabama, Mobile, Alabama, USA
Correspondence: Jianing Han, Department of Physics, University of South Alabama, Mobile, Alabama 36688, USA.

Received: September 1, 2023 Accepted: September 29, 2023 Online Published: October 1, 2023
doi:10.5539/apr.v15n2p173 URL: https://doi.org/10.5539/apr.v15n2p173

Abstract
Fano profiles are caused by the interference between the discrete states and continuum. It is a very common phenomenon in multi-electron Rydberg states, such as the Rydberg states of group II elements in the periodic table. It often leads to autoionization due to the fact that a discrete state couples with an autoionizing state. Unlike the typical asymmetric line shape, here we report a symmetric unusual Fano line shape that has been predicted. In addition, this profile is caused by molecular states or polymer states instead of multi-electron atomic states. Moreover, it is shown that the fano profile caused by the multi-electron polymer states does not necessarily lead to autoionization. We propose that the Fano profile studied is caused by the interference between discrete levels and the multipole-multipole coupled continuum, or energy band.

Keywords: Fano profile, Rydberg atom, two-photon, multipole-multipole interactions, dipole-dipole interactions, van der Waals interactions

1. Introduction

Fano profile has been observed since many decades ago (Beutler H., 1935), and the theoretical explanation was done by diagonalizing the Hamiltonian, including the discrete states and continuous states (Fano U., 1961). The basic idea of the theory is that the line shape is caused by the interference between two channels, an open channel (the continuous states) and a closed channel (the discrete states). Fano profiles have been continuously studied over the years. Here are a few examples of those studies. High-resolution Vacuum Ultraviolet (VUV) has been used to study the Fano profile of the Ba atoms and other multi-electron systems (ConneradeJ. P., 1992, Maeda K. et. al., 1992). A fano profile caused by a one-photon and a three-photon process interference has been investigated (Lounis B., 1992). The resonance attenuation can be explained by including the relation between the profile parameters and atomic matrix elements (Shore B. W., 1967). Magneto-Optical Rotation (MOR) has been observed in a Beutler-Fano profile (Connerade J. P., 1991, Connerade J. P., 1988, Mitchell A. C. G. et. al., 1971). Multiphoton ionization through Fano theory has been examined (Armstrong L. et. al., 1975). It was predicted that an asymmetric Fano-type magnetoplasmon resonance is observable in Bose-Fermi mixtures (Boev M. V. et. al., 2016). Recently, Fano profile has been studied in ultracold group I atomic gases both theoretically and experimentally in low principal quantum number states (Krems R. V. et. al., 2002, Lisdat C. et. al., 2002, Li Y. et. al., 2019, Pham K. et. al., 2022). However, the profile in highly excited states (Gallagher T. F., 1994) hasn't been reported. In this article, we focus on the Fano profile detected in highly excited states of cold Rb Rydberg atoms. Unlike previous isolated multi-electron atomic systems, we propose that the multipole-multipole coupled polymer system could lead to the observation of the Fano profile. In other words, the Fano profile in this case is caused by the interference between the isolated state and the multipole-multipole coupled continuum.

The research conducted has many potential applications. For instance, this can be used to study molecular autoionization. If a discrete molecular state couples with an autoionizing state, this will lead to autoionization. In addition, ionized states can be used to study plasma. Therefore, this study can be used to study plasma formation. Moreover, since the research studied is based on quantum mechanics, this can be used to study quantum physics. Many applications are based on excited states, such as quantum gates, and Fano profile may play a role in those applications. Quantum entanglement, quantum sensing, and quantum information storage also need to take into account the interference between isolated states and multipole-multipole coupled continuum.

2. Theory

With a magnetic field, the Fano profile can be modified to the following form (Fano U., 1961, Connerade J. P., 1992, Connerade J. P., 1988, Mitchell A. C. G. et. al., 1971):

$$\chi(x) = \frac{e^2 N f l \alpha}{mc(1+q^2)}\left(\frac{(q^2-1)(x^2-\Delta^2)+4q\Gamma x}{(x^2-\Delta^2)^2+4\Gamma^2 x^2}\right), \tag{1}$$

where q is the shape or profile index of the resonance, which depends on both the initial and final states. $\Delta^2 = \Gamma^2 + \alpha^2$, and $\alpha = \frac{eB}{4\pi mc}$. The magnetic field is set to zero. $x = \nu - \nu_0$, and ν_0 is the resonant frequency, and ν is the microwave frequency added to the system. In this article, we scale the profile to fit the experimental data.

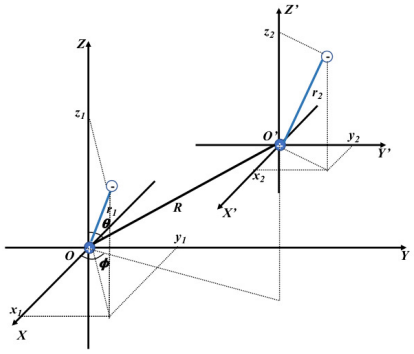

Figure 1: x_1, y_1, and z_1 are the projection of r_1, the distance between the outer electron and the ion core of the bottom atom, on the X, Y and Z axis. Similarly, x_2, y_2, and z_2 are the projection of r_2, the distance between the outer electron and the ion core of the top atom, on the X', Y' and Z' axis. θ is the angle between R and the Z axis, where R is the distance between the two atoms. ϕ is the angle between the projection of R on the $X - Y$ plane and the X axis.

Many previous studies have shown that the coupling of the isolated states with the autoionization states, or free states, leads to the Fano profile. In this experiment, we specifically monitored the free charge signal. When the Fano profile was observed, there were no free charges present, which indicates that such profiles are not caused by the interference between isolated states and the autoionizing states. In this article, we will show that the continuum is caused by the multipole-multipole coupled energy bands. We will show that as the number of atoms increases, the multipole-multipole coupled levels increase. Specifically, we use the two-atom and three-atom cases as examples. In reality, there are many atoms in the atomic sample; therefore, the energy is continuous. We consider up to $\frac{1}{R^5}$ terms. Dipole-dipole, dipole-quadrupole, and quadrupole-quadrupole interactions are included in this calculation. Dipole-octopole interactions are proportional to $\frac{1}{R^5}$; however, there is no octopole moment in the case considered; therefore, dipole-octopole interactions are excluded in this calculation. Below are the three-dimensional expressions for those interactions.

$$\begin{aligned} V_{dd} = \frac{e^2}{4\pi\epsilon_0 R^3}[&x_1x_2 + y_1y_2 + z_1z_2 \\ &- 3(sin\theta cos\phi x_1 + sin\theta sin\phi y_1 + cos\theta z_1)(sin\theta cos\phi x_2 + sin\theta sin\phi y_2 + cos\theta z_2)]; \end{aligned} \tag{2}$$

$$\begin{aligned} V_{dq} = -\frac{e^2}{4\pi\epsilon_0 R^4}[&3(sin\theta cos\phi x_2 + sin\theta sin\phi y_2 + cos\theta z_2)(x_1x_2 + y_1y_2 + z_1z_2) \\ &+ \frac{3}{2}(sin\theta cos\phi x_1 + sin\theta sin\phi y_1 + cos\theta z_1)(x_2^2 + y_2^2 + z_2^2) \\ &- \frac{15}{2}(sin\theta cos\phi x_1 + sin\theta sin\phi y_1 + cos\theta z_1)(sin\theta cos\phi x_2 + sin\theta sin\phi y_2 + cos\theta z_2)^2]; \end{aligned} \tag{3}$$

$$\begin{aligned} V_{qq} = \frac{e^2}{4\pi\epsilon_0 R^5}\{&\frac{3}{4}(x_1^2 + y_1^2 + z_1^2)(x_2^2 + y_2^2 + z_2^2) + \frac{3}{2}(x_1x_2 + y_1y_2 + z_1z_2)^2 \\ &- \frac{15}{4}[(sin\theta cos\phi x_1 + sin\theta sin\phi y_1 + cos\theta z_1)^2(x_2^2 + y_2^2 + z_2^2) \\ &+ (x_1^2 + y_1^2 + z_1^2)(sin\theta cos\phi x_2 + sin\theta sin\phi y_2 + cos\theta z_2)^2] \\ &- 15[(sin\theta cos\phi x_1 + sin\theta sin\phi y_1 + cos\theta z_1)(sin\theta cos\phi x_2 + sin\theta sin\phi y_2 + cos\theta z_2) \\ &(x_1x_2 + y_1y_2 + z_1z_2)] \\ &+ \frac{105}{4}[(sin\theta cos\phi x_1 + sin\theta sin\phi y_1 + cos\theta z_1)^2(sin\theta cos\phi x_2 + sin\theta sin\phi y_2 + cos\theta z_2)^2]\}. \end{aligned} \tag{4}$$

where x_1, y_1, x_1, x_2, y_2, z_2, θ, and ϕ are shown in Fig. 1.

The interaction between atom 1 and atom 2 is named as V_{12}. The interaction between three atoms is

$$V = V_{12} + V_{23} + V_{31}, \tag{5}$$

where V_{23} is the interaction between atom 2 and atom 3, and V_{31} is the interaction between atom 3 and atom 1.

3. Experiment

This experiment was carried out in an ultracold gas (Wineland D. J. et. al., 1978, Neuhauser W., 1978, William W. D., 1987, Chu S. et. al, 1985, Lett P. D. et. al. 1988, Ketterle W, 2002, Cornell E. A., 2002). The experimental setup is discussed in our earlier work. Briefly, a Magneto-Optical Trap is created by three pairs of retroreflected circularly polarized laser beams, and a repump laser is used to compensate for the decay of the trapped atoms. One improvement made over previous experiments is that the locking time of the trapping and repump lasers is much longer than the ones used in previous experiments. In addition, we are now able to manipulate the atoms using microwaves. The cold $5p_{3/2}$ atoms are then excited to highly excited states, 36s in this case. A microwave is used to excite the atoms from the 36s state to the 37s state. The highly excited states are then ionized by a field ionization pulse, or selective field ionization (SFI) (Gallagher T. F., 1977). The ionized ions are collected by a pair of microchannel plates (MCPs), which will result in a voltage signal. The voltage signal is imported to an oscilloscope. The oscilloscope traces are then recorded and analyzed by a computer. The excitation scheme and timing of this experiment are shown in Fig. 2, where $t_1 = 650$ ns, $t_2 = 1$ μs, and $t_3 = 500$ ns. The rising time of the field ionization pulse is 5 μs.

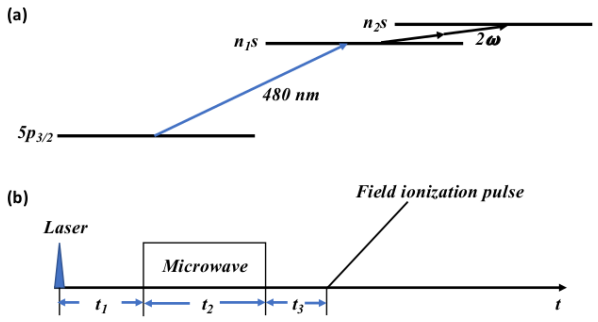

Figure 2: (a) The excitation scheme. (b) The timing of this experiment.

4. Results and Discussion

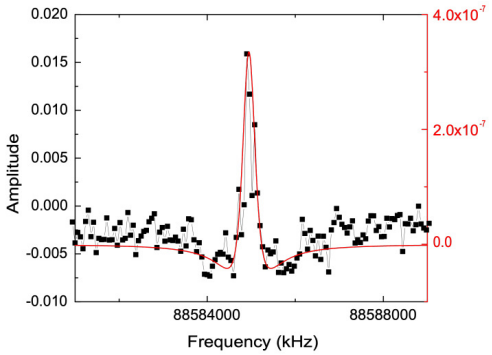

Figure 3: One microwave scan of the 36s to 37s two-photon transition. The bottom-left plot with black squares (■) is experimental data. The bottom-right plot with the red solid line (—) is theoretical data (Connerade J. P., 1988).

.

Fig. 3 shows a microwave scan of the 36s to 37s two-photon transition. We use a square microwave pulse, which causes the small side peaks due to the Fourier transform to frequency space of a square pulse in time. The power of the pulse is about a π pulse. Unlike the typical assymmetric Fano profile, the line shape in Fig. 3 is symmetric, which has been predicted (Connerade J. P., 1988). We then fit the data with a Fano profile, the red solid curve. It is shown

that the experimental data and the calculated data match very well. The shape index, q, and the magnetic field, B, are both set to be zero in the red solid curve. We interpret this as the interference between a single energy level with the multipole-multipole coupled continuum. As the density of the sample gets higher and higher, the $36p$ state signal caused by multipole-multipole interactions, which shows up at the same position as the $37s$ signal in the field ionization signal, increases, which makes it harder to see the profile. The slight broadening to the repulsive side of the spectrum of the high-density data is caused by van der Waals interactions.

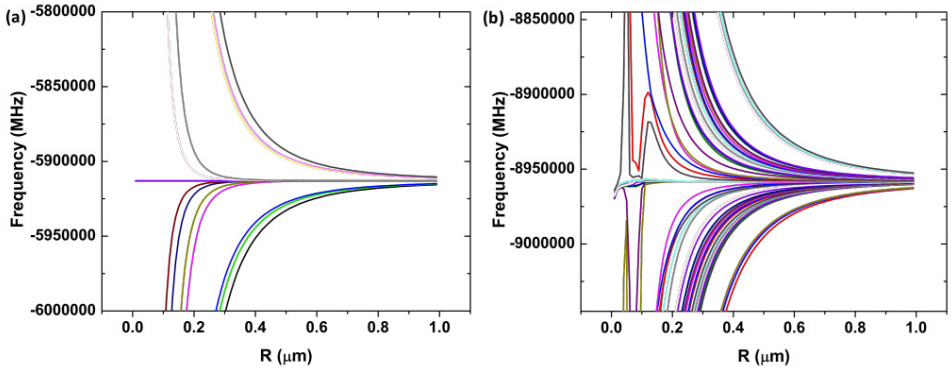

Figure 4: (a) Two body, $36s37s$ and $36p_{3/2}36p_{3/2}$, interaction energy levels. (b) Three body, $36s36s37s$ and $36s36p_{3/2}36p_{3/2}$, interaction energy levels.

The fact that we didn't see free charges in this experiment indicates that the isolated state is not coupled to autoionizing free states. We interpret this as the interference between isolated states and the few-body multipole-multipole coupled continuum. Below is an example to show where the continuum could come from. Fig. 4 shows the calculated energy level for two bodies and three bodies. Fig. 4(a) is the energy levels of the $36s37s$ dimer states and the energetically close states, $36p_{3/2}36p_{3/2}$ states. In these calculations, the exchange symmetry is considered. For example, both $36s_{1/2,1/2}37s_{1/2,1/2}$ and $37s_{1/2,1/2}36s_{1/2,1/2}$ are considered. We considered all the m levels, where m is the projection of the angular momentum on the z axis. Total 24 states are considered for the two-body case. Similarly, we add an additional $36s$ atom. The number of states considered for the three-body case is 120. We considered the interactions up to $\frac{1}{R^5}$, which include dipole-dipole, dipole-quadrupole, and quadrupole-quadrupole interactions. Since the dipole-octopole interactions are negligible in this particular case, we ignore the dipole-octopole interactions. It is shown that by adding an additional atom, the amount of energy levels increases significantly, and the interaction strength increases. In reality, the number of bodies, which interact with each other, is much greater than three. Therefore, energy bands rather than isolated energy levels are expected for ultracold Rydberg gases. In addition, the atomic sample is not uniform, and the atoms are randomly distributed, which will be more likely to create an energy continuum. For simplicity, we only considered a few states. The s states coupled with other energy levels through multipole-multipole interactions, which will contribute to the energy band. Moreover, as the interaction strength increases, the atomic states are no longer eigenstates of the system, and all states mix together. We did see potential wells for some configurations, which are favorable for molecular states at certain densities. In other words, this calculation doesn't exclude the possibility of creating molecules. In this article, we have focused on the energy continuum and ignored the molecular formation region.

5. Conclusion

Fano profiles have been studied in lower-level atoms in ultracold gases. In this article, we focused on the Fano profile among excited states. The Fano profile has been observed experimentally in ultracold Rydberg gases. Unlike the asymmetric line shape, here we report a symmetric unusual line shape. The fact that free charges were not present when the Fano profile was observed indicates that the isolated states were not coupled with the autoionization states or molecular autoionization states in this case. We qualitatively showed that the isolated states coupling with the few-body multipole-multipole coupled energy band led to the Fano profile observed. The limitation of the research is that this profile is only observable at a certain density range. For example, if the atomic sample is too dense, the profile is not observation. The observation of this type of profile opens up avenues for studying atom-atom interactions in an alternative way.

Acknowledgement

It is a pleasure to acknowledge the support from the Air Force Office of Scientific Research (AFOSR) and a previous award from the Army Research Office (ARO), and the University of South Alabama Faculty Development Council (USAFDC).

References

Armstrong, B. L. Jr., & Beers, B. L. (1975). Resonant multiphoton ionization via the Fano autoionization formalism. *Phys. Rev. A., 12,* 1903.

Beutler, H. (1935). *Z. Phys., 93,* 177.

Boev, S. M. V., Kovalev, V. M., & Savenko, I. G. (2016). Magentoplasmon Fano resonance in Bose-Fermi mixtures. *Phys. Rev. B., 94,* 241408(R).

Chu, S., Hollberg, L., Bjorkholm, J. E., Cable, A., & Ashkin, A. (1985). Three-dimensional viscous confinement and cooling of atoms by resonance radiation pressure. *Phys. Rev. Lett., 55,* 48.

Connerade, J. P. (1988). The theory of Faraday rotation in an autoionising resonance. *J. Phys. B: At. Mol. Opt. Phys., 21,* L551.

Connerade, J. P. (1991). Magneto-optical rotation in an autoionizing line. *J. Phys. B: At. Mol. Opt. Phys., 24,* L51.

Connerade, J. P. (1992). *J. Phys. II France, 2,* 757.

Cornell, E. A., & Wieman, C. E. (2002). Nobel Lecture: Bose-Einstein condensation in a dilute gas, the first 70 years and some recent experiments. *Rev. Mod. Phys, 74,* 875.

Fano, U. (1961). *Phys. Rev., 124,* 1866.

Gallagher, T. F., Humphrey, L. M., Cooke, W. E., Hill, R. M., & Edelstein, S. A. (1977). *Phys. Rev. A, 16,* 1098.

Gallagher, T. F. (1994). *Rydberg atoms.* Cambridge University Press, Cambridge.

Ketterle, W. (2002). Nobel lecture: When atoms behave as waves: Bose-Einstein condensation and the atom laser. *Rev. Mod. Phys, 74,* 1131.

Krems, D. R. V., & Dalgarno, A. (2002). *Phys. Rev.A, 66,* 012702.

Lett, P. D., Watts, R. N., Westbrook, C. I., Phillips, W. D., Gould, P. L., & Metcalf, H J. (1988). Observation of Atoms Laser Cooled below the Doppler Limit. *Phys. Rev. Lett., 61,* 169.

Li, Y.-Q., Feng, G.-S., Wu, J.-Z., Ma, J., Deb, B., Pal, A., Xiao, L.-T., & Jia, S.-T. (2019). *Phys. Rev. A, 99,* 022702.

Lounis, T. B., & Cohen-Tannoudji, C. (1992). *J. Phys. II France, 2,* 579.

Maeda, K., Ueda, K., Namioka, T., & Ito, K. (1992). *Phys. Rev. A., 45,* 527.

Mitchell, A. C. G., & Zemanski, M. W. (1971). *Resonance Radiation and Excited Atoms.* Cambridge University Press, Cambridge.

Neuhauser, W., Hohenstatt, M., Toschek, P., & Dehmelt, H. (1978). Optical-Sideband cooling of visible atom cloud confined in parabolic well. *Phys. Rev. Lett., 41,* 233.

Pham, K.-L., Gallagher, T. F., Pillet, P.,Lepoutre, S., & Cheinet, P. (2022). *PRX Quantum, 3,* 020327.

Phillips, W. D., & Metcalf, H. J. (1987). Cooling and trapping atoms. *Scientific America, 256,* 50.

Pillet Ch. Lisdat, N. Vanhnecke, D. Comparat, & P. Pillet, (2002). *Eur. Phys. J. D 21,* 299.

Shore, B. W. (1967). Scattering Theory of Absorption-Line Profiles and Refractivity. *Rev. Mod. Phys., 39,* 439.

Wineland, D. J., Drullinger, J. E., & Walls, F. L. (1978). Radiation-Pressure cooling of bound resonant absorbers. *Phys. Rev. Lett., 40,* 1639.

Copyrights